



Dynamic and synergistic influences of air temperature and rainfall on general flowering in a Bornean lowland tropical forest

Masayuki Ushio^{1,2,3}  | Yutaka Osada⁴ | Tomo'omi Kumagai⁵ | Tomonori Kume⁶ | Runi anak Sylvester Punga⁷ | Tohru Nakashizuka⁸ | Takao Itioka⁹ | Shoko Sakai² 

¹Hakubi Center, Kyoto University, Kyoto, Japan

²Center for Ecological Research, Kyoto University, Otsu, Japan

³PRESTO, Japan Science and Technology Agency, Kawaguchi, Japan

⁴Graduate School of Life Science, Tohoku University, Sendai, Japan

⁵Graduate School of Agricultural and Life Sciences, The University of Tokyo, Tokyo, Japan

⁶Kasuya Research Forest, Kyushu University, Fukuoka, Japan

⁷Research, Development and Innovation Division, Forest Department Sarawak, Kuching, Malaysia

⁸Research Department, Research Institute for Humanity and Nature, Kyoto, Japan

⁹Graduate School of Human and Environmental Studies, Kyoto University, Kyoto, Japan

Correspondence

Masayuki Ushio, Hakubi Center, Kyoto University, 606-8501 Japan.
Email: ong8181@gmail.com

Shoko Sakai, Center for Ecological Research, Kyoto University, 520-2113 Japan.
Email: shokosakai@ecology.kyoto-u.ac.jp

Funding information

Japan Society for the Promotion of Science, Grant/Award Number: 16H04830; Kyoto University

Abstract

Supra-annually synchronized flowering events occurring in tropical forests in Southeast Asia, known as general flowering (GF), are “spectacular and mysterious” forest events. Recently, studies that combined novel molecular techniques and model-based theoretical approaches suggested that cool temperature and drought synergistically drove GF. Although these advanced our understanding of GF, it is still difficult to know whether the individual-based molecular measurements and model-based mathematical representations reasonably well capture the complex and dynamic GF processes at the community level. In the present study, we collected a 17-year set of community-wide phenology data from Lambir Hills National Park in Borneo, Malaysia, and analyzed it using a model-free approach, empirical dynamic modeling (EDM), which does not rely on specific assumptions about the underlying mechanisms, to overcome and complement the previous limitations. We found that GF in the region is driven synergistically, not independently, by cool air temperature and drought, which is consistent with the previous studies. More importantly, our model-free approach showed for the first time that effects of cumulative meteorological variables on GF changed over time. The time-varying influences of meteorological variables on GF imply that the relationship between GF and meteorological variables might be influenced by other factors such as plant/soil nutrient resource dynamics. Our study provides a novel insight about the mechanism underlying the spectacular tropical forest event GF, and future studies integrating advanced mathematical/statistical frameworks, long-term and large spatial scale ecosystem monitoring and molecular phenology data are promising for achieving better understanding and forecasting of GF events in Southeast Asia.

KEYWORDS

Borneo, empirical dynamic modeling, general flowering, Lambir Hill national park, time series, tropical forest

Masayuki Ushio is the recipient of the 22nd Denzaburo Miyadi Award.

This is an open access article under the terms of the Creative Commons Attribution-NonCommercial License, which permits use, distribution and reproduction in any medium, provided the original work is properly cited and is not used for commercial purposes.

© 2019 The Authors. *Ecological Research* published by John Wiley & Sons Australia, Ltd on behalf of The Ecological Society of Japan

1 | INTRODUCTION

Supra-annually synchronized flowering events occurring in tropical forests in Southeast Asia, known as general flowering (GF) or community-level masting, are “spectacular and mysterious” forest events (Ashton, Givnish, & Appanah, 1988; Sakai, 2002; Sakai et al., 2006). GF is a masting phenomenon unique to Asian dipterocarp forests, and it is unique in involving the synchronization of flowering/fruitletting across diverse plant groups (Ashton et al., 1988; Sakai, 2002). Plants including most dipterocarps and many other plant groups flower over roughly a 3-month period, and produce numerous of flowers (and subsequently, fruits) during the event. Conversely, flowers are rare between GF events especially in the canopy layer, while many understory herbs and treelets may flower more frequently. Therefore, GF plays an important role in plant reproduction and regeneration. In addition to its influence on plant communities, GF also influences forest animal communities, including pollinators and seed predators, through trophic cascades because plants provide a large amount of nutrient resources to forest animals (Curran & Leighton, 2000; Iku et al., 2017; Itioka et al., 2001; Nakagawa, Miguchi, Sato, Sakai, & Nakashizuka, 2007; Te Wong, Servheen, Ambu, & Norhayati, 2005). As a result, GF influences overall dynamics of forest ecosystems, and thus understanding GF mechanisms and predicting GF events are important for tropical forest conservation and management.

Because GF occurs over a large spatial scale and across numerous plant groups, it is reasonable to assume that major drivers of GF are environmental rather than local biotic interactions. However, environmental cues that triggered GF have not been fully understood despite intense efforts of theoretical and empirical ecologists. Researchers have traditionally investigated potential environmental cues using observation and simple correlation analysis. For example, using simple correlations between environmental variables and the proportion of flowering and fruiting tree individuals, Sakai et al. (2006) and Brearley, Proctor, Nagy, et al. (2007) independently suggested that irregular drought caused by El Niño southern oscillation (ENSO) events trigger GF. Other researchers suggested that low air temperature and nutrient resources (e.g., phosphorus) are important cues (Ashton et al., 1988; Ichie, 2013), but detailed investigations of how these factors influence GF are still ongoing.

Recently, several research groups addressed this question by using advanced molecular techniques and theoretical approaches. For example, Kobayashi et al. (2013) investigated gene expression patterns of buds of *Shorea beccariana* before and during the flowering event in Lambir Hills National Park in Borneo, Malaysia. They found that expression levels of flowering-related genes, drought-

responsive genes and sucrose-induced genes showed significant changes before flowering. Chen et al. (2017) analyzed 13 years of weekly flowering records collected in Pasoh Research Forest in Peninsular Malaysia using a mathematical modeling approach, and showed that drought and cool temperature synergistically best explain the timing of flowering events of *Shorea* species. Furthermore, Yeoh et al. (2017) used molecular phenology data collected from two *Shorea* species in forests near Forest Research Institute Malaysia in the state of Selangor, Malaysia, to answer the question. The mathematical modeling of the molecular phenology data suggested that cool air temperature and drought synergistically influence the gene expression pattern of the *Shorea* (Yeoh et al., 2017). Molecular phenology, also known as the “ecological transcriptome” is the analysis of plant transcriptome time series collected from natural ecosystems, and has recently been recognized as a powerful tool to understand causes and molecular mechanisms of plant phenology in nature (Aikawa, Kobayashi, Satake, Shimizu, & Kudoh, 2010; Kudoh, 2016; Yeoh et al., 2017). These recent studies that utilized novel techniques suggested that several factors, rather than a single factor, synergistically act as triggers of GF in Southeast Asia.

Although these advanced and integrated approaches have helped to advance our understanding of GF events, there still are several important limitations. First, although mathematical modeling that explicitly constructed model structures reasonably well explained GF events and/or gene expression patterns in the previous studies, it is difficult to know whether the mathematical formulations (i.e., model equations) reasonably well represented the complex and dynamic processes involved in GF. In other words, misspecifications of the model structure may lead us to wrong conclusions, but unfortunately, specifying model structures correctly is often difficult for complex, natural ecological dynamics. In addition, because the model-based approach utilizes a priori and fixed assumptions on the relationships between variables, it is often difficult to capture the flexible, time-varying interactions between variables. Second, in terms of gene expression data, measuring gene expression patterns from tropical tree species is still time-, labor- and money-consuming work, and thus, the molecular phenology data can often be collected from only a few individuals. Considering that GF is a community-wide phenomenon, analyzing community-wide data would provide important insights and reveal different aspects of GF mechanisms.

In the present study, we collected 17 years of community-wide phenology data from Lambir Hills National Park in Borneo, Malaysia, and analyzed it using a model-free approach to overcome and complement the limitations of earlier approaches. The long-term phenology data were collected by direct visual census (Sakai et al., 2006); the monitored

plant individuals were first identified and the number of flowering plant individuals was counted fortnightly during June 1993 to January 2011 (i.e., the index of GF was “the proportion of flowering plant individuals in the census”). Then, the time series data were analyzed using empirical dynamic modeling (EDM) (Deyle, May, Munch, & Sugihara, 2016; Sugihara et al., 2012; Ye et al., 2015). Instead of assuming a set of equations that govern the dynamics, EDM recovers system dynamics from the time series trajectory (for a brief introduction, see Chang, Ushio, & Hsieh, 2017 and Methods section). This unique feature enables us to analyze time series without assuming a specific model structure, and thus is often suitable for analyzing and predicting dynamics of complex, time-varying systems such as natural ecosystems. In the time series analysis, we particularly focused on the influences of air temperature and rainfall because these two factors have been suggested to be dominant environmental factors that trigger GF in many studies (Ashton et al., 1988; Brearley et al., 2007; Chen et al., 2017; Kobayashi et al., 2013; Sakai et al., 2006; Yeoh et al., 2017). The community-wide and model-free analysis, which we present here, was lacking in the previous studies, and we tested whether the “cool air temperature and drought hypothesis” was validated using our approach.

2 | MATERIALS AND METHODS

2.1 | Study site

The study site is in a lowland dipterocarp forest at Lambir Hills National Park, Borneo (4°20'N, 113°50'E, 150–250 m a. s.l.) (Roubik, Sakai, & Karim, 2005). Rainfall data were collected at the Bukit Lambir Station of the Department of Irrigation and Drainage (DID), Sarawak, Malaysia, within the park ~3 km northwest of the study site. From 1985 to 2003, the average annual rainfall was ~2,700 mm, and the annual rainfall ranged from 2,000 to 3,800 mm. Seasonal variation was significant but low, and the area occasionally had droughts with biological consequences (Harrison, 2000; Itioka & Yamauti, 2004; Kishimoto-Yamada et al., 2009; Nakagawa et al., 2000; Nakagawa, Ushio, Kume, & Nakashizuka, 2019).

2.2 | Time series of general flowering

Plants were observed using a canopy observation system (tree towers and walkways) constructed at the center of the Canopy Biology Plot (8 ha, 200 × 400 m) (Roubik et al., 2005). The Canopy Biology Plot includes humult and udult soils (sandy clay, light clay, or heavy clay in texture), several ridges and valleys, and closed (mature-stage) forests and canopy gaps. In each census, presence or absence of flowers on focal plants was recorded fortnightly (Sakai et al., 2006).

After excluding plants with missing values, records of 204 individuals from June 6th, 1993 to January 5th, 2011 were used in the time series. The index of GF in the present study was “the proportion of flowering plant individuals in the census”, which was calculated as follows: (the number of flowering plant individuals in the census)/(the number of total plant individuals in the census [= always 204 during the census term]). The monitored plant individuals belong to 38 families, 80 genera, 133 species, and dominant families are as follows: Dipterocarpaceae ($N = 74$; genera *Shorea*, *Dipterocarpus*, *Dryobalanops* and *Vatica* were included), Euphorbiaceae ($N = 23$), Leguminosae ($N = 17$), Annonaceae ($N = 8$), Burseraceae ($N = 8$), Myristicaceae ($N = 7$) and other families ($N = 67$). General flowering events were observed seven times during the census period (Figure 1a). During the 17 years and 7 months census period, the total number of time points used for the general flowering time series was 423 (i.e., fortnightly census for 211 months).

2.3 | Meteorological time series

From 1993 to 1998, temperature was monitored every 30 min using a temperature/humidity sensor (E7050–10, Yakogawa Weathac Corp., Tokyo, Japan) on a tower 35 m above the ground located in the Canopy Biology Plot (Sakai et al., 2006). From 2000 to 2011, temperature was monitored every 10 min using a thermohygrograph (HMP35A, Visala Co., Helsinki, Finland) installed at the height of 76 m on a crane tower located ~0.5 km from the plot (Kume et al., 2011). For rainfall from 1993 to 1999, data collected daily at the Bukit Lambir Station of the Department of Irrigation and Drainage (DID), Sarawak, Malaysia, within the park ~3 km northwest of the study site, was used. From 2000 to 2011, rainfall was monitored using a tipping bucket rain gauge (RS102, Ogasawara Keiki, Tokyo, Japan) at the top of the crane, 85.8 m above the ground (Kume et al., 2011).

In the analysis, we used the observed meteorological data when it was available. When observed data were not available, the data were complemented by a reanalyzed and gridded four-dimensional meteorology data set, JRA-55 (Kobayashi et al., 2015) for the nearest grid point 3°45'N, 113°45'E. In total, air temperature data at 62 time points (with 2-week intervals) were not available among the total 423 time points and were complemented by using the simulated air temperature data (a major missing period for air temperature data were from October 1998 to January 2001; 31 time points). For rainfall data, there were no missing data and thus only observed data were used for the analyses. Although the study site is an aseasonal tropical rain forest, there are variations in daily

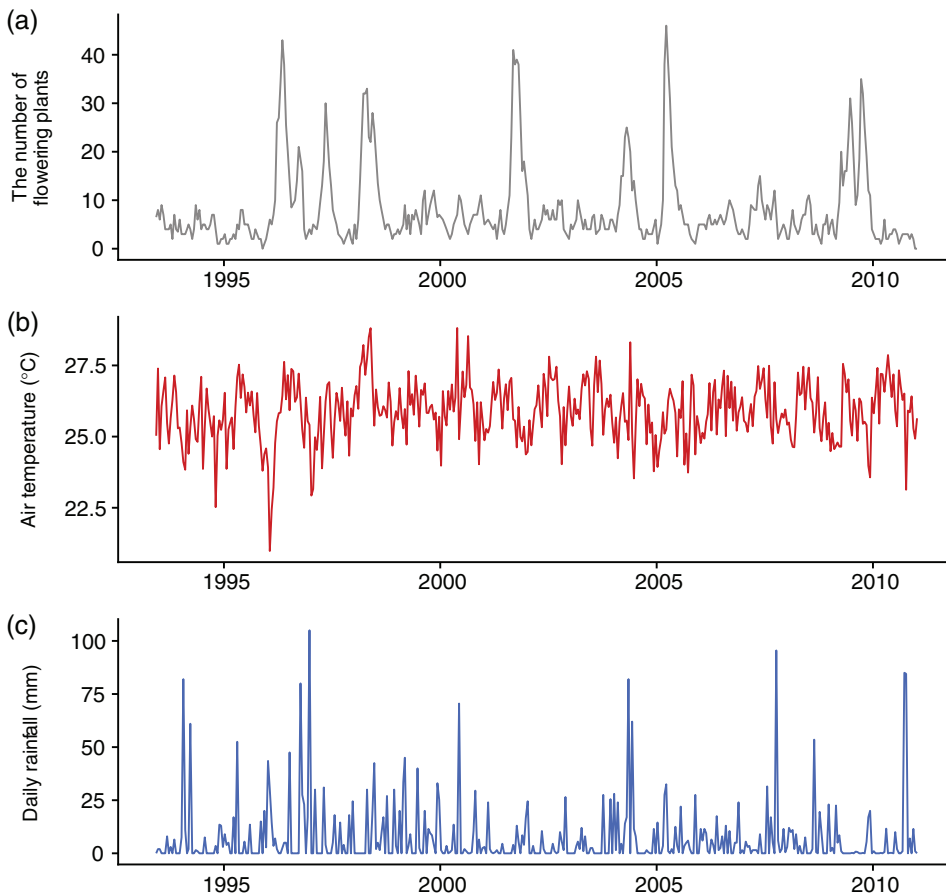


FIGURE 1 Time series of general flowering and climate variables. (a) The number of flowering plant individuals. The total number of monitored plant individuals was 204. (b) Daily mean air temperature ($^{\circ}\text{C}$). (c) Daily rainfall (mm)

mean air temperature and rainfall (Figure 1b,c; Kume et al., 2011).

2.4 | Calculations of cumulative air temperature and rainfall

Meteorological variables were first converted to daily values (i.e., daily mean air temperature and daily rainfall) during the census term (i.e., from June 1993 to January 2011), and the cumulative values for the daily variables were calculated. To examine the most influential cumulative duration, we calculated the cumulative values from 7-days to 364-days with 7-day intervals. Thus, we had 52 values for cumulative calculation \times two meteorological variables = 104 variables to be examined by empirical dynamic modeling (see the section below).

2.5 | State space reconstruction and framework of empirical dynamic modeling

Time series can be defined as any set of sequential observations of the system state, and the dynamic behaviors can be delineated as a trajectory of a state over time in a multi-dimensional state space by plotting time series. Time series taken from ecosystems (i.e., ecological time series) can be

used to trace out trajectories of the system, which provide a large amount of information on ecosystem dynamics. For example, if one has performed sequential observations on a three-species ecological system, for example, grasses (primary producer), rabbits (consumer) and foxes (predator), then the dynamics of the three-species system can be reconstructed by plotting time series of grasses, rabbits, and foxes along the x , y , and z axis, respectively, in a three-dimensional state space. The motion of the three-dimensional vectors can be understood as the system behavior.

In a natural ecosystem, however, it is almost impossible to collect time series of all potentially important variables involved in a target system. Fortunately, Takens (1981) offered a theoretical basis to solve this problem: a mathematical theorem, Takens' embedding theorem, demonstrated that a shadow version of the attractor (motion of vectors in a state space) can be reconstructed by a single observed time series (for example, the time series of grasses, x). In other words, delineation of trajectories, originally constructed using multiple variables, can be possible even if a time series is available only for a single variable (Sauer, Yorke, & Casdagli, 1991; Takens, 1981). To embed such a single time series (with an equal sampling interval), vectors in the putative phase space are formed from time-delayed values of the time series, $\{x(t), x(t - \tau), x(t - 2\tau), \dots, x(t -$

$[E - 1]\tau\}$, where E is the embedding dimension, and τ is the time lag. This procedure, the reconstruction of the original dynamics, is known as state space reconstruction (SSR) (Deyle & Sugihara, 2011; Takens, 1981).

Recently developed tools for nonlinear time series analysis, which are specifically designed to analyze state-dependent behavior of dynamical systems, called Empirical Dynamic Modeling (EDM), are rooted in SSR (Deyle et al., 2016; Dixon, Milicich, & Sugihara, 1999; Kitayama, Ushio, & Aiba, 2018; Sugihara, 1994; Sugihara & May, 1990; Ushio et al., 2018; Ye, Beamish, et al., 2015; Ye, Deyle, Gilarranz, & Sugihara, 2015; Ye & Sugihara, 2016). These methods do not assume any set of equations governing the system, and thus are suitable for analyzing complex systems, for which it is often difficult to make reasonable a priori assumptions about their underlying mechanisms. Instead of assuming a set of specific equations, EDM recovers the dynamics (and potentially, underlying mechanism) directly from time series data using SSR, and is thus particularly useful for forecasting ecological time series, which are otherwise often difficult to forecast.

2.6 | Convergent cross mapping between general flowering and meteorological variables

In order to detect causation between GF and meteorological variables, we used convergent cross mapping (CCM) (Sugihara et al., 2012). An important consequence of the SSR theorems is that if two variables are part of the same dynamical system, then the reconstructed state spaces of the two variables will represent topologically the same attractor (with a one-to-one mapping between reconstructed attractors). Therefore, it is possible to predict the current state of a variable using time lags of another variable. We can look for the signature of a causal variable in the time series of an effect variable by testing whether there is a correspondence between their reconstructed state spaces (i.e., cross mapping). This cross-map technique can be used to detect causation between variables. Cross-map skill can be evaluated by either a correlation coefficient (ρ), or mean absolute error (MAE) or root-mean-square error (RMSE) between observed and predicted values by cross mapping. In the algorithm of CCM, the library length, which is defined by the number of points in the reconstructed state space of an effect variable, plays an important role. The maximum library length is described as follows: (the maximum library length) = (the number of points in the time series of an effect variable) - (E of an effect variable - 1). Once the state space is reconstructed, one can choose a subset of points in the state space from which the nearest neighbors of a target vector will be searched. For example, if one wants to detect causation from air temperature to GF, a target vector, $\{GF[t^*]$,

$GF[t^* - 1], \dots, GF[t^* - (E - 1)]\}$, will be used to predict a corresponding value of air temperature at time t^* (where E and t^* indicate best embedding dimension of GF and a target time point, respectively). As the number of points in the subset (i.e., the library length) increases, the trajectory defining the attractor fills in, which results in close nearest neighbors and declining estimation error (e.g., smaller RMSE) if two variables are causally related (i.e., convergence). The convergence is a practical criterion of causality, and thus the method is called convergent cross mapping (CCM).

In the present study, cross mapping from one variable to another was performed using simplex projection. How many time lags ($\tau = 1$ throughout the analyses) are taken in SSR (i.e., best embedding dimension; E) is determined by simplex projection using RMSE as an index of forecasting skill. Note that the time series analyzed are standardized to have zero mean and unit variance, and thus RMSE usually ranges from 0 to 1 (RMSE can sometimes be >1 , but can never be <0). Based on the results of simplex projection, the best embedding dimension was estimated to be six, and thus $E = 6$ was used for GF time series throughout the analyses. More detailed algorithms about simplex projection and cross mapping can be found in previous studies (Chang et al., 2017; Sugihara et al., 2012; Sugihara & May, 1990).

In CCM analysis, we also considered the time lag between GF time series and potential causal time series (i.e., cumulative meteorological variables). This can be done by using “lagged CCM” (Ye, Deyle, et al., 2015). For normal CCM, correspondence between reconstructed state space (i.e., cross-mapping) is checked using the same time point. In other words, information embedded in an effect time series at time t may be used to predict the state of a potential causal time series at time t . This idea can easily be extended to examine time-delayed influence between time series by asking the following question: is it possible to predict the state of a potential causal time series at time $t - tp$ (tp is a time delay) by using information embedded in an effect time series at time t ? Ye, Deyle, et al. (2015) showed that lagged CCM is effective to determine the effect time delay between variables. In the present study, we examined the effect time delay from 0 days to 336 days with 14-day intervals. Examining the effect time delay with shorter time intervals (e.g., 7-day intervals) was not possible because the original GF time series are taken fortnightly.

In the present study, the significance of CCM is judged by comparing convergence in the cross-map skill of Fourier surrogates and original time series. More specifically, first, 1,000 surrogate time series for one original time series are generated. Fourier surrogates were generated by randomizing the phases of a Fourier transform using `rEDM::make_surrogate_ebisuzaki()` function implemented in `rEDM` package (version 0.7.1; Ye, Clark, Deyle, & Munch 2018). Second, the convergence of the cross-map skill is calculated for

1,000 surrogate time series and the original time series. Specifically, the convergence of the cross-map skill is calculated as the cross-map skills at the maximum library length minus that at the minimum library length (Sugihara et al., 2012), denoted by ΔRMSE in the present study. When performing cross-map from GF index to another variable, the maximum library length is 418 (= [the number of points in the GF time series] - $[E - 1]$). The minimum library length should theoretically be 0, but in practice, $E + 1$ (= 7) is often used to make a simplex around a target point. ΔRMSE should be negative if two variables are causally coupled. Again, the time series analyzed are standardized to have zero mean and unit variance, and ΔRMSE in the present study ranged from -0.154 to 0.008. If less than 50 surrogates (i.e., < 5% of the surrogates) have a smaller ΔRMSE than that of the original time series, the cross mapping is judged as significant.

In the present study, we first tested which combinations of time-delay and the number of days for cumulative value calculation have the strongest causality for the GF index using ΔRMSE as an index of the strength of causality. After the identification of the “best” combination, we tested the significance of the causality of the best combination using the surrogate approach explained above. In addition, to facilitate comparisons of the surrogate-based P values, we calculated the P values for other combinations of time-delay and the number of days for cumulative value calculation. The results are shown in the supplementary figure.

2.7 | Multivariate S-map method

The multivariate S-map (sequential locally weighted global linear map) method allows quantification of dynamic (i.e., time-varying) interactions (Deyle et al., 2016; Sugihara, 1994). Consider a system that has E different interacting variables, and assume that the state space at time t is given by $\underline{x}(t) = \{x_1(t), x_2(t), \dots, x_E(t)\}$. For each target time point t^* , the S-map method produces a local linear model C that predicts the future value $x_j(t^* + p)$ from the multivariate reconstructed state space vector $\underline{x}(t^*)$. That is,

$$\hat{x}_1(t^* + p) = C_0 + \sum_{j=1}^E C_j x_j(t^*)$$

where $\hat{x}_1(t^* + p)$ is a predicted value of x_1 at time $t^* + p$, and C_0 is an intercept of the linear model. The linear model is fit to the other vectors in the state space. However, points that are close to the target point, $\underline{x}(t^*)$, are given greater weighting. The model C is the singular value decomposition (SVD) solution to the equation

$$B = A \cdot C$$

where B is an n -dimensional vector (n is the number of observations) of the weighted future values of $x_j(t_i)$ for each historical point, t_i , given by

$$B_i = w(\|\underline{x}(t_i) - \underline{x}(t^*)\|) x_1(t_i + p)$$

and A is then $n \times E$ dimensional matrix given by

$$A_{ij} = w(\|\underline{x}(t_i) - \underline{x}(t^*)\|) x_j(t_i)$$

The weighting function w is defined by

$$w(d) = \exp\left(-\frac{\theta d}{\bar{d}}\right)$$

which is tuned by the nonlinear parameter $\theta \geq 0$ and normalized by the average distance between $\underline{x}(t^*)$ and the other historical points,

$$\bar{d} = \frac{1}{n} \sum_{i=1}^n \|\underline{x}(t_i) - \underline{x}(t^*)\|$$

$\|\underline{x} - \underline{y}\|$ is the Euclidian distance between two vectors in the E -dimensional state space. Note that the model C is separately calculated (and thus potentially unique) for each time point, t . As recently shown, C , the coefficients of the local linear model, are a proxy for the interaction strength between variables (Deyle et al., 2016).

In the same way as with simplex projection and CCM, the performance of the multivariate S-map was also measured by RMSE between observed and predicted values by the S-map (i.e., leave-one-out cross validation). As mentioned in the CCM section, the time series analyzed by the S-map method are also standardized to have zero mean and unit variance, and thus RMSE usually ranges from 0 to 1.

2.8 | Computation and result visualization

Simplex projection, S-map and CCM were performed using “rEDM” package (version 0.7.1) (Ye et al., 2018; Ye, Beamish, et al., 2015), results were visualized using “ggplot2” (Wickham, 2009), “cowplot” (Wilke, 2017), and “ggsci” (Xiao, 2018) packages. All statistical analyses were performed in the free statistical environment R3.4.4 (R Core Team, 2018).

2.9 | Code and data availability

Our time series data and computing codes include unpublished works that involved multiple researchers and institutions. Therefore, the data and codes are currently not

deposited in a public archive such as Dryad, GitHub or Zenodo. They will eventually be available as a Data paper and/or original research papers. At present, all data and code are available upon reasonable request.

3 | RESULTS AND DISCUSSION

3.1 | Detection of causal factors of general flowering

According to the lagged CCM, 7-days cumulative air temperature with 28-days delay and 7-days cumulative rainfall with 42-days delay most strongly determine the number of flowering plant individuals in the Lambir forest plot (Figure 2). In the analysis, we relied on ΔRMSE , but qualitatively similar results were obtained even when using $\Delta\rho$ and ΔMAE (Figure S1). In addition, 7-day cumulative air temperature with 28-days delay and 7-days cumulative rainfall with 42-days delay were statistically significant causal factors based on the Fourier surrogate analysis ($p < .05$, Figure S2). Including 7-days cumulative air temperature with 28-days delay and 7-days cumulative rainfall with 42-days delay in the multivariate S-map improved the forecasting skill (RMSE and ρ) of GF compared with the univariate model and models with air temperature only or rainfall only (Figure 3; $\text{RMSE}_{\text{Full}} - \text{RMSE}_{\text{Flower}} = -0.0042$, $\text{RMSE}_{\text{Flower + temp}} - \text{RMSE}_{\text{Flower}} = -0.0006$, and $\text{RMSE}_{\text{Flower + rain}} - \text{RMSE}_{\text{Flower}} = -0.0028$; $\rho_{\text{Full}} - \rho_{\text{Flower}} = .0015$, $\rho_{\text{Flower + temp}} - \rho_{\text{Flower}} < 0$, and $\rho_{\text{Flower + rain}} - \rho_{\text{Flower}} = .0011$). Furthermore, the improvement of the forecasting skill of the “Full” model is better than the sum of the improvements of the forecasting skills of the “Flower + temp” or “Flower + rain” model, indicating that the improvement of the forecasting skill of the “Full” model cannot be explained by the additive effect of air temperature and rainfall. These results suggest that air temperature and rainfall synergistically, not independently, influence GF in the study site.

In addition to 7-days cumulative air temperature with 28-days delay and 7-days cumulative rainfall with 42-days delay, other cumulative values with different delays may have causal influences on the number of flowering plant individuals in the forest (Figures 2 and S1,S2). This suggests that detailed mechanisms of the influences of air temperature and rainfall may include several different pathways, for example, air temperature in one day may consequently influence the number of flowering plant individuals in different days. If this is the case, there may be two different

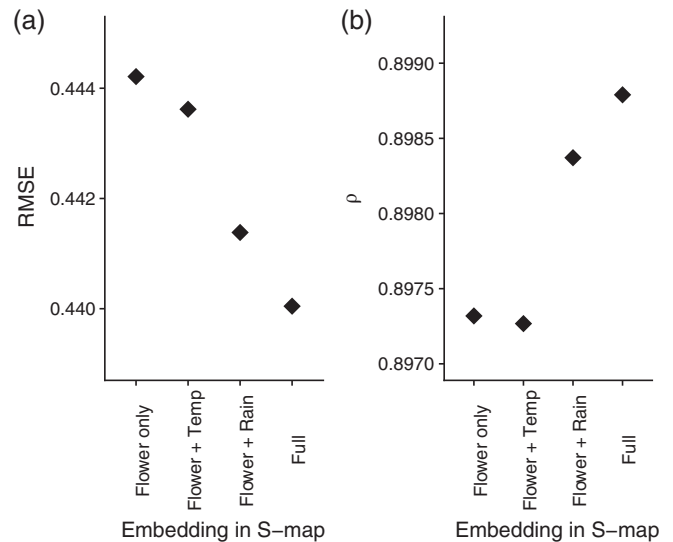
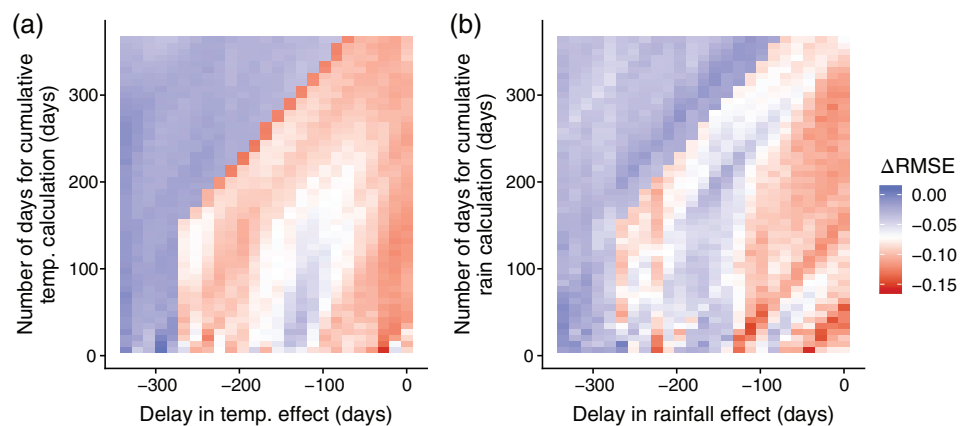


FIGURE 3 Improvements of forecasting skill by the univariate/multivariate S-map method. (a) Root mean square error (RMSE) by the S-map methods that used four different sets of embeddings. “Flower only” indicates that only GF index was used to forecast GF index (i.e., embedding = $\{GF_t, \dots, GF_{t-5}\}$). “Flower + Temp” and “Flower + Rain” indicates embedding was $\{GF_t, \dots, GF_{t-4}, \text{Cum.Temp}\}$ and $\{GF_t, \dots, GF_{t-4}, \text{Cum.Rainfall}\}$, respectively. “Full” indicates that the embedding was $\{GF_t, \dots, GF_{t-3}, \text{Cum.Temp}, \text{Cum.Rainfall}\}$ (b) Correlation coefficient (ρ) by the S-map methods that used four different sets of embeddings. Note that, as the best embedding dimension of GF was estimated to be 6, the number of coordinates in the multivariate S-map is fixed as six

FIGURE 2 Results of convergent cross mapping (CCM). Improvement of forecasting skill (measured by root-mean-square error [ΔRMSE]) by CCM for different combinations of effect time-delay and number of days for cumulative calculation of air temperature (a) and rainfall (b)



approaches to model the GF: (a) including all causal climate variables, or clustering similar variables, in the model, or (b) including the most influential climate variables (i.e., the 7-days cumulative climate variables with delays) in the model. The first approach could most appropriately describe the GF, but at the same time, including all potential cumulative and delay values makes a model extremely complex and reduces the model interpretability. On the other hand, the second approach is often rather simple and thus more easily interpretable. Also, the previous related studies applied an approach that identified and included a single or a few best parameters (Chen et al., 2017; Yeoh et al., 2017). Therefore, in the present study, we focus on the influences of 7-days

cumulative air temperature with 28-days delay and 7-days cumulative rainfall with 42-days delays as representative and integrated climate indices that influence GF in the subsequent analysis in order to improve the interpretability of the results and to facilitate comparison with the previous studies.

3.2 | Influences of air temperature and rainfall

Influences of 7-days cumulative air temperature and rainfall were quantified by calculating the coefficients (C_j , see Methods) of the multivariate S-map method that showed the

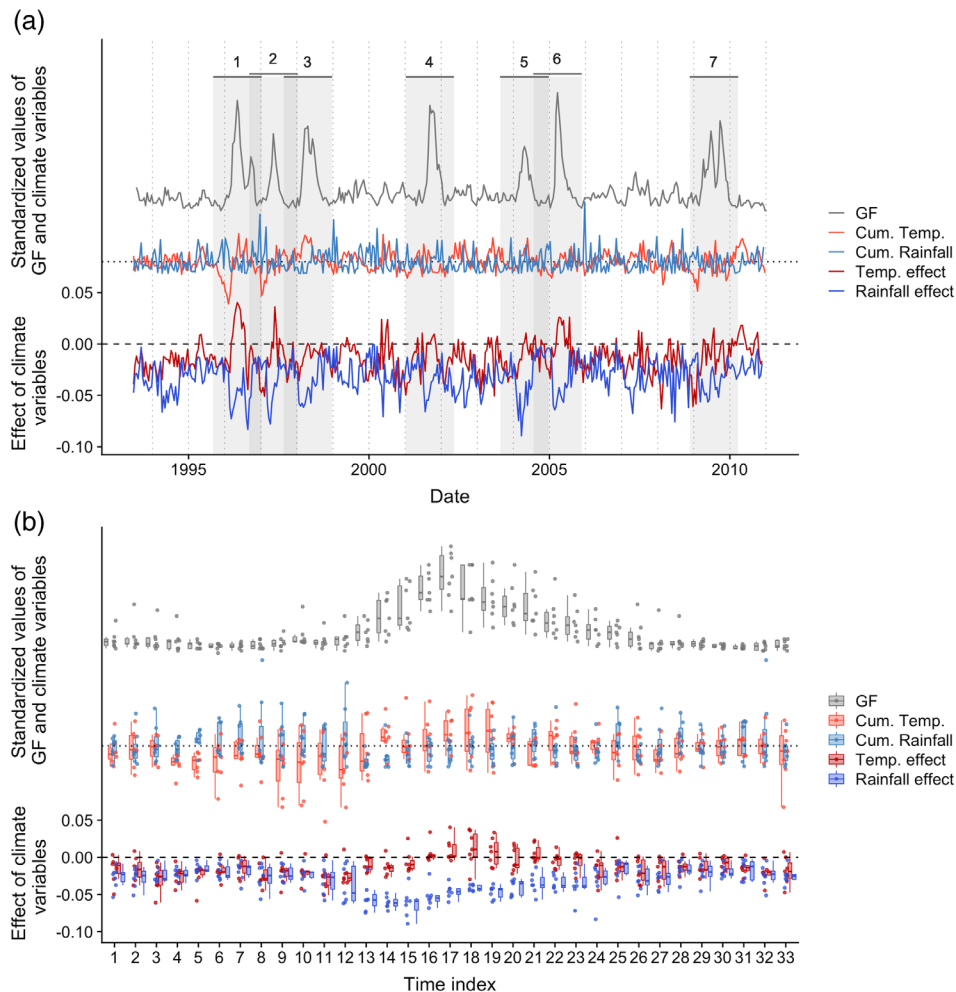


FIGURE 4 Time series of GF, cumulative climate variables and their influence on GF. (a) Standardized GF and cumulative temperature and rainfall were plotted. Values on the y-axis are only for effects of climate variables. Dotted and dashed horizontal lines indicate mean value for cumulative climate variables and zero for effects of climate variables, respectively. Different line colors indicate different time series categories. Vertical dotted lines correspond to one-year. Vertical shaded regions indicate the GF periods and were used to make panel b. Seven GF periods, that is, (1) 1995/9–1997/1, (2) 1996/9–1998/1, (3) 1997/8–1998/12, (4) 2001/1–2005/8, (5) 2003/8–2004/12, (6) 2004/7–2005/12 and (7) 2008/11–2010/3, were extracted for panel b. The numbers above the shaded regions indicate the order of GF events extracted. (b) Time-windows of 8-months before and 6-months after each 3-months GF period (i.e., 17-months time-window) were extracted from panel a and plotted using box and jitter plots. One time index corresponds to 2-weeks. Dotted and dashed horizontal lines indicate mean value for cumulative climate variables and zero for effects of climate variables, respectively. Note that effects of cumulative temperature and rainfall are delayed by 28 and 42 days, respectively. For example, cumulative rainfall (and its effect) at time index 4 influence GF at time index 6

best forecasting skill (i.e., “Full” model in Figure 3). In general, 7-days cumulative air temperature and rainfall have negative influences on GF (Figure 4a, red and blue solid lines), indicating that decreased air temperature and drought increase the number of flowering plant individuals in the forest, which is consistent with the previous studies (Chen et al., 2017; Kobayashi et al., 2013; Sakai et al., 2006; Yeoh et al., 2017). However, though in general air temperature and rainfall have negative influences on GF, air temperature sometimes has positive influences on GF, that is, increased air temperature increases the number of flowering plant individuals in the forest (Figure 4a; the red line sometimes exceeds zero indicated by the dashed line).

To examine the detailed patterns of the influences of air temperature and rainfall on GF, a 17-month time window around each GF event (i.e., 8 months before GF, 3 months GF period and 6 months after GF) was extracted (Figure 4b; time windows around seven GF periods were used, that is, the periods of 1995/9–1997/1, 1996/9–1998/1, 1997/8–1998/12, 2001/1–2005/8, 2003/8–2004/12, 2004/7–2005/12 and 2008/11–2010/3, indicated by gray shading in Figure 4a). According to the visualization, GF, air temperature and rainfall and their influences on GF showed consistent patterns across the seven GF events (Figure 4b). The GF event generally started 2.5–3 months (i.e., time indices 12–13) before its peak (at time index 17 in Figure 4b), and decreased air temperature was found during ca. 4 months before the initiation of GF (time indices 4–12 in Figure 4b, orange points and boxplots). Therefore, a first cue of a GF event might be decreased air temperature rather than drought. Interestingly, increases in rainfall that coincided with decreases in air temperature were found ca. 4 months before the initiation of GF (time indices 5–6 in Figure 4b, skyblue points and boxplots), which might be a previously overlooked sign of GF initiation. Then, in the GF increasing period, drought positively and strongly influenced the number of flowering plant individuals (time indices 12–16 in Figure 4b, skyblue and blue points and boxplots). After the GF peak, slightly increased air temperature contributed to the maintenance of GF (time indices 17–20 in Figure 4b, orange and red points and boxplots). Interestingly and importantly, these patterns were generally consistent across the seven GF events, and thus monitoring air temperature and rainfall may help to forecast GF.

To search for more detailed patterns, we examined the relationships between GF, air temperature, rainfall and their influences using scatter plots (Figure 5). According to the analysis, there may be a threshold of cumulative rainfall to induce GF. GF happens only when 7-day cumulative rainfall values are below ~100 mm (Figure 5a). This suggests that drought may be a necessary condition, but not a sufficient condition, for GF. On the other hand, there is no clear and linear relationship between GF and air temperature

(Figure 5b), suggesting that air temperature is, though significant, a less important causal factor of GF than drought. In addition, during GF periods, the influence of drought is stronger than that during other periods, and there are linear relationships between climate variables and their influences on GF (Figure 5c,d). This suggests that the effects of climate factors on GF are not constant, but can change depending on the states of a forest ecosystem. Also, more severe drought, and/or lower air temperature have stronger influences on GF, and thus, they may induce a larger GF event.

3.3 | Comparisons with previous studies using different approaches and factors not incorporated in the present study

Using a 17-year, fortnightly direct visual observation of GF and EDM, we showed that air temperature and rainfall synergistically and dynamically drive GF at a community-level in the tropical forest in Lambir Hills National Park in Borneo, Malaysia. This finding is consistent with the recent studies that suggested synergistic influences of air temperature and rainfall (Chen et al., 2017; Yeoh et al., 2017). Responses of expression levels of drought- and/or air temperature-related genes may be an important individual-level basis for the initiation of GF, as found in previous molecular studies (Kobayashi et al., 2013), but elucidating how these molecular-level responses scale up to community-level responses will need further studies.

Previous studies analyzed flowering records by assuming that there are threshold temperature and rainfall for signal accumulation, and suggested that “signal accumulation” (equivalent to our “cumulative values”) ranged from 54 to 90 days, and “days for flower development” (equivalent to our “effect time delay”) ranged from 43 to 96 days (Chen et al., 2017), and these values were longer than our findings which showed that 7-days cumulative air temperature with a 28-days effect delay and 7-days cumulative rainfall with a 42-days effect delay are the most influential climate variables. Reasons for these differences could be multifold: (a) modeling approach, (b) the characteristics of the time series analyzed, and (c) the criterion used to identify the most influential climate variables. First, these differences may be partly due to differences in modeling approaches. When using a model-based approach, estimated parameter values depend on the model structure. In other words, if the model structure changes, estimated parameter values (i.e., days for signal accumulations and days for flower development) may change. Second, the differences may also be due to the characteristics of the time series analyzed. In Chen et al. (2017), species-specific flowering records were analyzed, but our time series are community-wide flowering records. Therefore, estimated cumulative days and effect delays were

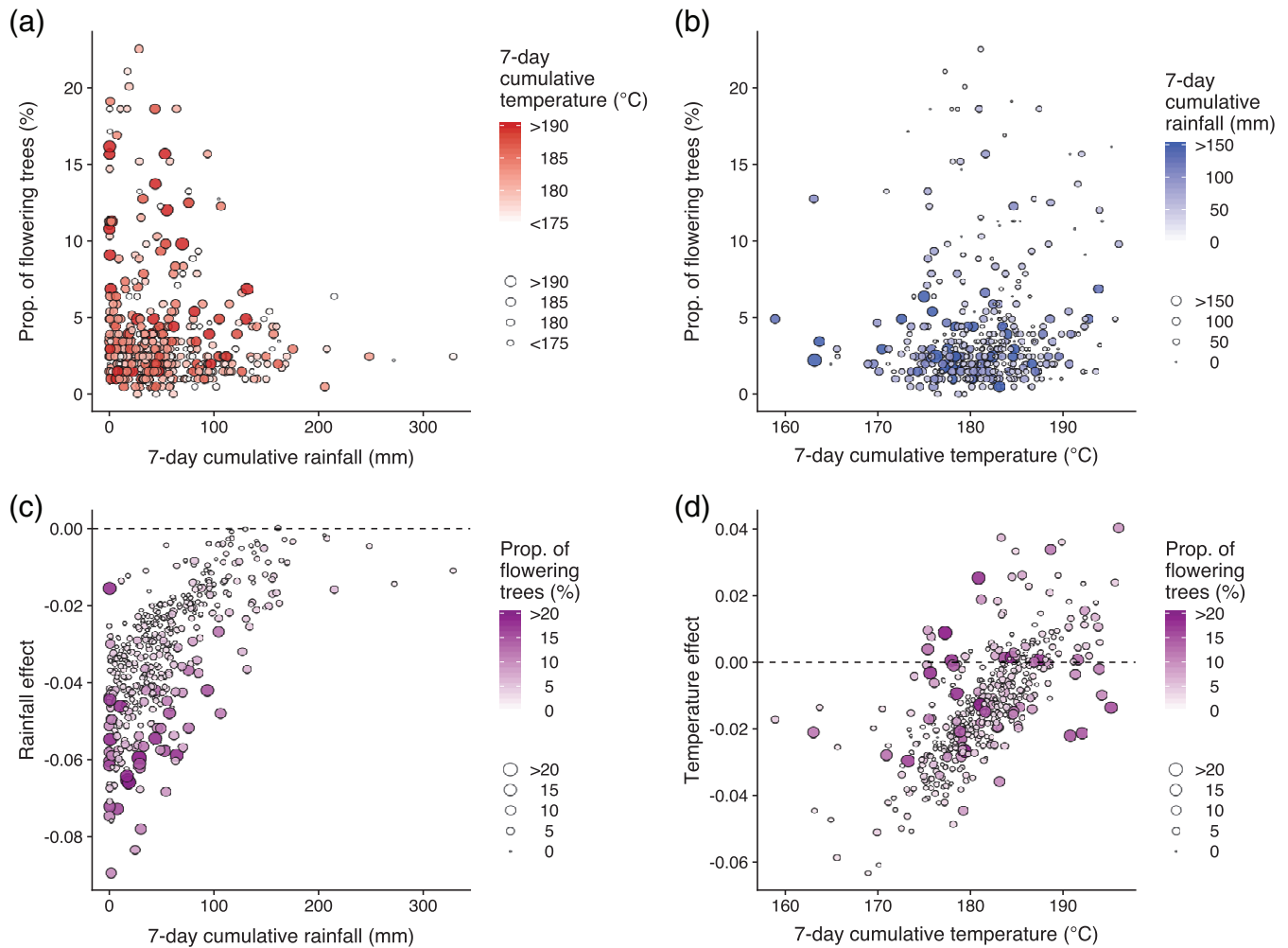


FIGURE 5 The relationships between the proportion of flowering plants, cumulative climate variables and effects of cumulative climate variables. (a) The relationship between the proportion of flowering plants and 7-day cumulative rainfall. Color density and point size indicate 7-day cumulative temperature. (b) The relationship between the proportion of flowering plants and 7-day cumulative temperature. Color density and point size indicate 7-day cumulative rainfall. (c) The relationship between 7-day cumulative rainfall and effects of cumulative rainfall. Color density and point size indicate the proportion of flowering plants. (d) The relationship between 7-day cumulative temperature and effects of cumulative temperature. Color density and point size indicate the proportion of flowering plants

community-wide (or community-averaged) ones, and thus they may be different from species-specific parameters. Third, although our analysis focused on the most influential cumulative values and effect delays, longer cumulative values and effect delays are also suggested to be factors that influence GF (Figure 2 and S1, S2), and the previous studies might have detected such longer values as the most influential values due to the differences in the modeling approach. Altogether, it is not surprising that we found several differences in the estimated parameter values, considering the differences in modeling approaches and time series characteristics.

In addition to those important differences between our study and the previous studies, we note that our approach, that is, CCM, does not explicitly distinguish direct and indirect causal effects. In other words, the 7-days cumulative

climate variables we identified may represent other factors that influence GF directly (e.g., actual vapor pressure and soil water content), and the number of days for cumulative calculations as well as effect delays of such factors may be different from air temperature and rainfall. This is particularly important when one tries to investigate more detailed biological/physiological mechanisms. For example, the 7-days cumulative climate variables do not necessarily drive gene expressions of plants directly; rather, there may be more direct environmental factors which are causally associated with GF and the 7-days cumulative climate variables. Unfortunately, our present approach is not able to identify specific biological/physiological mechanisms of GF. Future studies that investigate detailed biological/physiological mechanisms of GF will be needed to identify the factors that influence GF directly.

3.4 | State dependent influences of air temperature and rainfall on the general flowering

One of the interesting findings of our study is that effects of air temperature and rainfall may change depending on the states of the forest ecosystem (Figures 4 and 5), which was not pointed out in the previous studies. The time-varying effects of climate may be reasonable because factors other than climate (e.g., tree physiological conditions such as the level of internal nutrient resources) are suggested to be an important factor to determine the flowering timing (Ichie, 2013). For example, when sufficient phosphorus and/or nitrogen are not stored in the tree body, climate cues, for example, drought and low air temperature, would not induce flowering. Also, the best embedding dimension of GF time series was estimated to be 6 ($E = 6$), suggesting that there is a possibility that the number of potential factors that influence GF might be more than two if the influences of climate variables on GF are sufficiently linear (Takens, 1981). Incorporating other potential factors (e.g., plant and soil resource dynamics, tree root-fungal associations and other meteorological variables) might further improve the skill of forecasting GF, which would contribute to better understanding of GF mechanisms.

4 | CONCLUSIONS

Using a long-term phenology monitoring data set and empirical dynamic modeling, we showed that GF in the forest in Lambir Hills National Park is synergistically driven by decreased air temperature and drought. These findings are consistent with those of previous monitoring, molecular and statistical studies (Chen et al., 2017; Kobayashi et al., 2013; Sakai et al., 2006; Yeoh et al., 2017). Several studies, including the present study, suggested that cumulative meteorological variables, rather than instantaneous values, with some effects of delays may drive GF, but robust estimations of the values of parameters for the accumulation and delay effects will need further studies. Unlike previous studies, the present study showed for the first time that the effect of meteorological variables on GF might change over time, which implies that some other factors such as plant/soil nutrient resource dynamics may be involved in GF. Integrating novel mathematical/statistical frameworks, long-term and large spatial scale ecosystem monitoring and large-scale molecular phenology is promising for better understanding and forecasting GF events in tropical forests in Southeast Asia.

ACKNOWLEDGMENTS

This study was conducted in accordance with memorandums of understanding signed in 2005 by the Sarawak Forestry Corporation (SFC, Kuching, Malaysia) and the Japan Research Consortium for Tropical Forests in Sarawak (JRCTS, Sendai, Japan), and in 2012 by the Sarawak Forest Department (SFD, Kuching, Malaysia) and JRCTS. We thank Mohd Shahbudin Sabki and other staff of SFD, Lucy Chong and other staff of SFC, and staff of Lambir National Park for their support for our study, and Chih-hao Hsieh for discussion about EDM. This study was financially supported by Grants-in-Aid (No. 16H04830 to S.S.) from the Japanese Ministry of Education, Science and Culture and the Hakubi project of Kyoto University.

CONFLICT OF INTEREST

The authors declare that they have no competing interests.

ORCID

Masayuki Ushio  <https://orcid.org/0000-0003-4831-7181>

Shoko Sakai  <https://orcid.org/0000-0002-4267-8405>

REFERENCES

- Aikawa, S., Kobayashi, M. J., Satake, A., Shimizu, K. K., & Kudoh, H. (2010). Robust control of the seasonal expression of the Arabidopsis FLC gene in a fluctuating environment. *Proceedings of the National Academy of Sciences of the United States of America*, *107*, 11632–11637. <https://doi.org/10.1073/pnas.0914293107>
- Ashton, P. S., Givnish, T. J., & Appanah, S. (1988). Staggered flowering in the Dipterocarpaceae: New insights into floral induction and the evolution of mast fruiting in the aseasonal tropics. *The American Naturalist*, *132*, 44–66. <https://doi.org/10.1086/284837>
- Brearley, F. Q., Proctor, J., Nagy, L., Dalrymple, G., & Voysey, B. C. (2007). Reproductive phenology over a 10-year period in a lowland evergreen rain forest of central Borneo. *Journal of Ecology*, *95*, 828–839. <https://doi.org/10.1111/j.1365-2745.2007.01258.x>
- Chang, C.-W., Ushio, M., & Hsieh, C. (2017). Empirical dynamic modeling for beginners. *Ecological Research*, *32*, 785–796. <https://doi.org/10.1007/s11284-017-1469-9>
- Chen, Y.-Y., Satake, A., Sun, I.-F., Kosugi, Y., Tani, M., Numata, S., ... Wright, S. J. (2017). Species-specific flowering cues among general flowering Shorea species at the Pasoh research Forest, Malaysia. *Journal of Ecology*, *106*, 586–598. <https://doi.org/10.1111/1365-2745.12836>
- Curran, L. M., & Leighton, M. (2000). Vertebrate responses to spatio-temporal variation in seed production of mast-fruiting Dipterocarpaceae. *Ecological Monographs*, *70*, 101–128. [https://doi.org/10.1890/0012-9615\(2000\)070\[0101:VRTSVI\]2.0.CO;2](https://doi.org/10.1890/0012-9615(2000)070[0101:VRTSVI]2.0.CO;2)
- Deyle, E. R., May, R. M., Munch, S. B., & Sugihara, G. (2016). Tracking and forecasting ecosystem interactions in real time. *Proceedings of the Royal Society B: Biological Sciences*, *283*, 20152258. <https://doi.org/10.1098/rspb.2015.2258>

- Deyle, E. R., & Sugihara, G. (2011). Generalized theorems for nonlinear state space reconstruction. *PLoS One*, *6*, e18295. <https://doi.org/10.1371/journal.pone.0018295>
- Dixon, P. A., Milicich, M. J., & Sugihara, G. (1999). Episodic fluctuations in larval supply. *Science*, *283*, 1528–1530.
- Harrison, R. D. (2000). Repercussions of El Niño: Drought causes extinction and the breakdown of mutualism in Borneo. *Proceedings of the Royal Society B: Biological Sciences*, *267*, 911–915. <https://doi.org/10.1098/rspb.2000.1089>
- Ichie, T. (2013). Dynamics of mineral nutrient storage for mast reproduction in the tropical emergent tree *Dryobalanops aromatica*. *Ecological Research*, *28*, 151–158.
- Iku, A., Itioka, T., Kishimoto-Yamada, K., Shimizu-kaya, U., Mohammad, F. B., Hossman, M. Y., ... Meleng, P. (2017). Increased seed predation in the second fruiting event during an exceptionally long period of community-level masting in Borneo. *Ecological Research*, *32*, 537–545. <https://doi.org/10.1007/s11284-017-1465-0>
- Itioka, T., Inoue, T., Kaliasang, H., Kato, M., Nagamitsu, T., Momose, K., ... Yamane, S. (2001). Six-year population fluctuation of the giant honey bee *Apis dorsata* (hymenoptera: Apidae) in a tropical lowland dipterocarp forest in Sarawak. *Annals of the Entomological Society of America*, *94*, 545–549. [https://doi.org/10.1603/0013-8746\(2001\)094\[0545:SYFOT\]2.0.CO;2](https://doi.org/10.1603/0013-8746(2001)094[0545:SYFOT]2.0.CO;2)
- Itioka, T., & Yamauti, M. (2004). Severe drought, leafing phenology, leaf damage and Lepidopteran abundance in the canopy of a Bornean Aseasonal tropical rain Forest. *Journal of Tropical Ecology*, *20*, 479–482.
- Kishimoto-Yamada, K., Itioka, T., Sakai, S., Momose, K., Nagamitsu, T., Kaliasang, H., ... Inoue, T. (2009). Population fluctuations of light-attracted chrysomelid beetles in relation to supra-annual environmental changes in a Bornean rainforest. *Bulletin of Entomological Research*, *99*, 217–227. <https://doi.org/10.1017/S000748530800624X>
- Kitayama, K., Ushio, M., & Aiba, S. (2018). Celestially determined annual seasonality of equatorial tropical rain forests. *bioRxiv*, *454058*, 1–14. <https://doi.org/10.1101/454058>
- Kobayashi, M. J., Takeuchi, Y., Kenta, T., Kume, T., Diway, B., & Shimizu, K. K. (2013). Mass flowering of the tropical tree *Shorea beccariana* was preceded by expression changes in flowering and drought-responsive genes. *Molecular Ecology*, *22*, 4767–4782. <https://doi.org/10.1111/mec.12344>
- Kobayashi, S., Ota, Y., Harada, Y., Ayataka, E., Masami, M., Hirokatsu, O., ... Kiyotoshi, T. (2015). The JRA-55 reanalysis: General specifications and basic characteristics. *Journal of the Meteorological Society of Japan Series II*, *93*, 5–48. <https://doi.org/10.2151/jmsj.2015-001>
- Kudoh, H. (2016). Molecular phenology in plants: In natura systems biology for the comprehensive understanding of seasonal responses under natural environments. *The New Phytologist*, *210*, 399–412. <https://doi.org/10.1111/nph.13733>
- Kume, T., Tanaka, N., Kuraji, K., Komatsu, H., Yoshifuji, N., Saitoh, T. M., ... Kumagai, T. (2011). Ten-year evapotranspiration estimates in a Bornean tropical rainforest. *Agricultural and Forest Meteorology*, *151*, 1183–1192. <https://doi.org/10.1016/j.agrformet.2011.04.005>
- Nakagawa, M., Miguchi, H., Sato, K., Sakai, S., & Nakashizuka, T. (2007). Population dynamics of arboreal and terrestrial small mammals in a tropical rainforest, Sarawak, Malaysia. *Raffles Bulletin of Zoology*, *55*, 389–395.
- Nakagawa, M., Tanaka, K., Nakashizuka, T., Ohkubo, T., Kato, T., Maeda, T., ... Seng, L. H. (2000). Impact of severe drought associated with the 1997–1998 El Niño in a tropical forest in Sarawak. *Journal of Tropical Ecology*, *16*, 355–367.
- Nakagawa, M., Ushio, M., Kume, T., & Nakashizuka, T. (2019). Seasonal and long-term patterns in litterfall in a Bornean tropical rainforest. *Ecological Research*, *34*, 31–39. <https://doi.org/10.1111/1440-1703.1003>
- R Core Team (2018) R: A Language and Environment for Statistical Computing. Vienna, Austria
- Roubik, D.W., Sakai, S., Karim, A.A.H. (2005) *Pollination ecology and the rain forest: Sarawak studies*. New York: Springer-Verlag.
- Sakai, S. (2002). General flowering in lowland mixed dipterocarp forests of south-East Asia. *Biological Journal of the Linnean Society*, *75*, 233–247. <https://doi.org/10.1046/j.1095-8312.2002.00016.x>
- Sakai, S., Harrison, R. D., Momose, K., Kuraji, K., Nagamasu, H., Yasunari, T., ... Nakashizuka, T. (2006). Irregular droughts trigger mass flowering in aseasonal tropical forests in asia. *American Journal of Botany*, *93*, 1134–1139. <https://doi.org/10.3732/ajb.93.8.1134>
- Sauer, T., Yorke, J. A., & Casdagli, M. (1991). Embedology. *Journal of Statistical Physics*, *65*, 579–616. <https://doi.org/10.1007/BF01053745>
- Sugihara, G. (1994). Nonlinear forecasting for the classification of natural time series. *Philosophical Transactions of the Royal Society A: Mathematical, Physical and Engineering Sciences*, *348*, 477–495. <https://doi.org/10.1098/rsta.1994.0106>
- Sugihara, G., May, R., Ye, H., Hsieh, C. H., Deyle, E., Fogarty, M., & Munch, S. (2012). Detecting causality in complex ecosystems. *Science*, *338*, 496–500. <https://doi.org/10.1126/science.1227079>
- Sugihara, G., & May, R. M. (1990). Nonlinear forecasting as a way of distinguishing chaos from measurement error in time series. *Nature*, *344*, 734–741. <https://doi.org/10.1038/344734a0>
- Takens, F. (1981). Detecting strange attractors in turbulence. In D. Rand & L.-S. Young (Eds.), *Lecture Notes in Mathematics* (Vol. 898, pp. 366–381). New York: Springer-Verlag.
- Te Wong, S., Servheen, C., Ambu, L., & Norhayati, A. (2005). Impacts of fruit production cycles on Malayan sun bears and bearded pigs in lowland tropical forest of Sabah, Malaysian Borneo. *Journal of Tropical Ecology*, *21*, 627–639. <https://doi.org/10.1017/S0266467405002622>
- Ushio, M., Hsieh, C., Masuda, R., Deyle, E. R., Ye, H., Chang, C. W., ... Kondoh, M. (2018). Fluctuating interaction network and time-varying stability of a natural fish community. *Nature*, *554*, 360–363.
- Wickham, H. (2009). *ggplot2: Elegant graphics for data analysis*. New York: Springer-Verlag.
- Wilke, C.O. (2017) Cowplot: Streamlined plot theme and plot annotations for “ggplot2”
- Xiao, N. (2018) ggsci: Scientific Journal and Sci-Fi Themed Color Palettes for “ggplot2”
- Ye, H., Beamish, R. J., Glaser, S. M., Grant, S. C. H., Hsieh, C. H., Richards, L. J., ... Sugihara, G. (2015). Equation-free mechanistic ecosystem forecasting using empirical dynamic modeling. *Proceedings of the National Academy of Sciences of the United States of America*, *112*, E1569–E1576. <https://doi.org/10.1073/pnas.1417063112>

- Ye, H., Clark, A., Deyle, E., Munch, S. (2018) *rEDM: Applications of empirical dynamic Modeling from time series*. <https://doi.org/10.5281/zenodo.1294063>
- Ye, H., Deyle, E. R., Gilarranz, L. J., & Sugihara, G. (2015). Distinguishing time-delayed causal interactions using convergent cross mapping. *Scientific Reports*, *5*, 14750.
- Ye, H., & Sugihara, G. (2016). Information leverage in interconnected ecosystems: Overcoming the curse of dimensionality. *Science*, *353*, 922 LP–925.
- Yeoh, S. H., Satake, A., Numata, S., Ichie, T., Lee, S. L., Basherudin, N., ... Tani, N. (2017). Unravelling proximate cues of mass flowering in the tropical forests of South-East Asia from gene expression analyses. *Molecular Ecology*, *26*, 5074–5085. <https://doi.org/10.1111/mec.14257>

SUPPORTING INFORMATION

Additional supporting information may be found online in the Supporting Information section at the end of this article.

How to cite this article: Ushio M, Osada Y, Kumagai T, et al. Dynamic and synergistic influences of air temperature and rainfall on general flowering in a Bornean lowland tropical forest. *Ecological Research*. 2020;35:17–29. <https://doi.org/10.1111/1440-1703.12057>